Journal of Wood Science

NOTE

Effect of side-chain length in lignin model compound on MnO$_2$ oxidation: comparison of oxidations between C$_6$-C$_2$- and C$_6$-C$_1$-type compounds

Shirong Sun and Tomoya Yokoyama[*]

Abstract

Monomeric C$_6$-C$_2$-type lignin model compounds with a *p*-hydroxyphenyl (**H**), guaiacyl (**G**), syringyl (**S**), or *p*-ethylphenyl (**E**) nucleus (1-phenylethanol derivatives) were individually oxidized by MnO$_2$ at a pH of 1.5 and room temperature. The results were compared with those of the corresponding C$_6$-C$_1$-type benzyl alcohol derivatives obtained in our recent report to examine the effect of the presence of the *β*-methyl group on the oxidation. The presence decelerated the oxidation regardless of the type of aromatic nucleus, although it did not change the order of the oxidation rates: **G** > **S** >> **H** > **E**. This deceleration results from the steric factor of the *β*-methyl group in the C$_6$-C$_2$-type compounds. The MnO$_2$ oxidations of the corresponding C$_6$-C$_2$-type compounds deuterated at their *α*-(benzyl)positions showed that the magnitudes of the kinetic isotope effects are smaller than those observed in the oxidations of the corresponding C$_6$-C$_1$-type compounds, regardless of the type of aromatic nucleus. These smaller magnitudes suggest that the presence of the *β*-methyl group shifts the initial oxidation mode of MnO$_2$ from direct oxidation of the benzyl position to one-electron oxidation of the aromatic nucleus. Only the **S**-type compounds afforded products via degradation of the aromatic nuclei.

Keywords: Aromatic cation radical, Benzoquinone, Manganese dioxide

Introduction

Oxidation, together with acidic and alkaline reactions, is a common method for chemical treatment in biomass conversion where delignification is targeted. We have focused on manganese dioxide (MnO$_2$) as an oxidant of lignin, owing to its easy handling and recyclability. MnO$_2$ is reduced to divalent manganese ion (Mn^{2+}) when used as an oxidant under acidic conditions, and Mn^{2+} can be reconverted to MnO$_2$ by oxygen oxidation under alkaline conditions. However, MnO$_2$ oxidation of lignin from a pure chemistry viewpoint has been examined in only a few studies [1, 2].

Our previous report showed that MnO$_2$ is a good delignifying agent and is appropriate for introduction at the prebleaching stage (oxygen delignification) [3]. When an oxygen delignification process is substituted with MnO$_2$ oxidation at a temperature of 70 ℃ and pH of 2.0 in a sulfate buffer solution after the middle stage, the delignification of hardwood unbleached kraft pulp progresses more than in the process without the substitution, while carbohydrates are damaged only slightly.

A common mode of MnO$_2$ oxidation is to oxidize a conjugated hydroxy group, such as allyl or benzyl alcohol, to the corresponding carbonyl group. This does not seem to contribute to depolymerization of lignin and delignification, and therefore the mechanism of MnO$_2$ oxidation
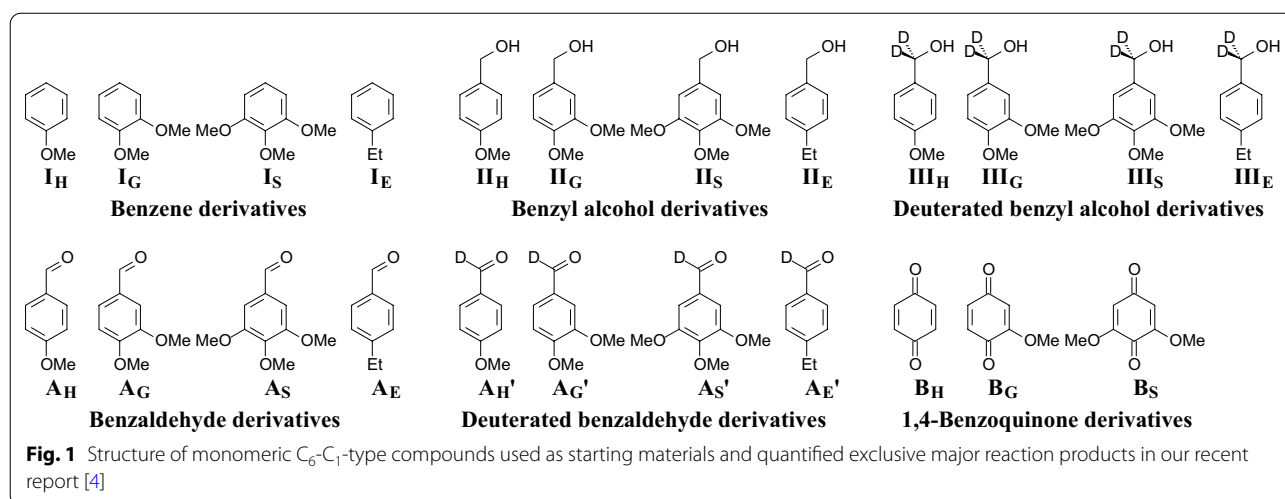
*Correspondence: yokoyama@woodchem.fp.a.u-tokyo.ac.jp
Laboratory of Wood Chemistry, Department of Biomaterial Sciences,
Graduate School of Agricultural and Life Sciences, The University of Tokyo,
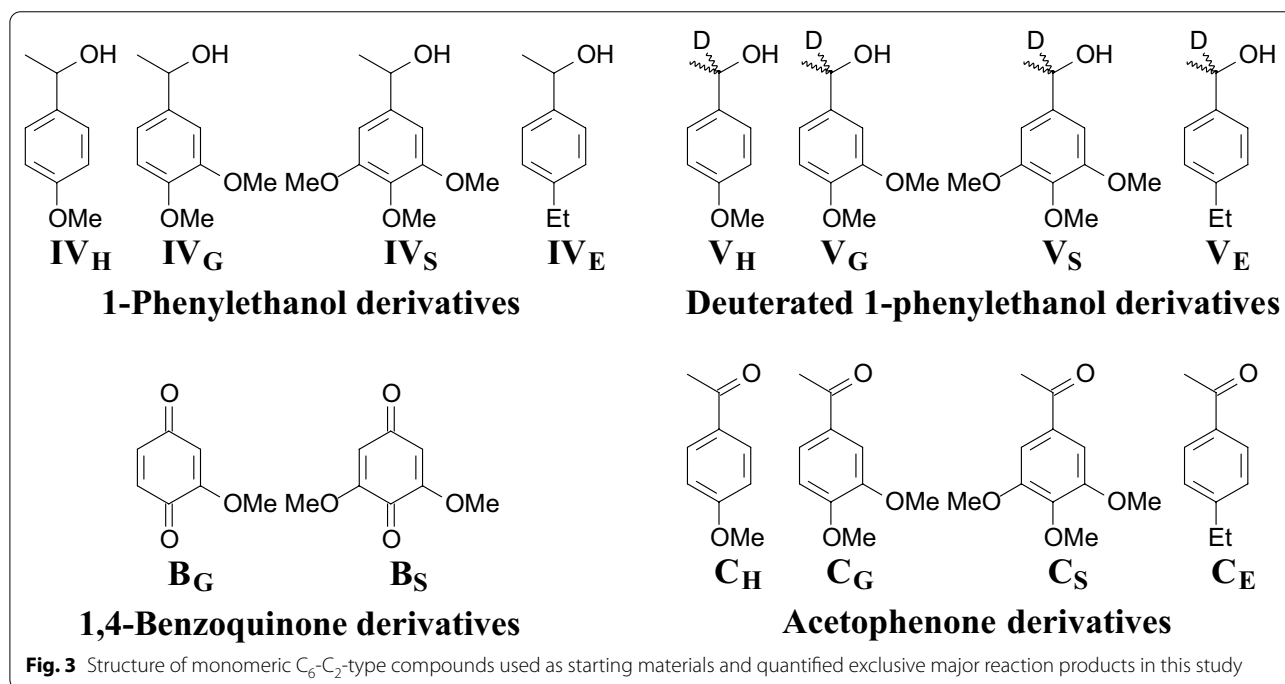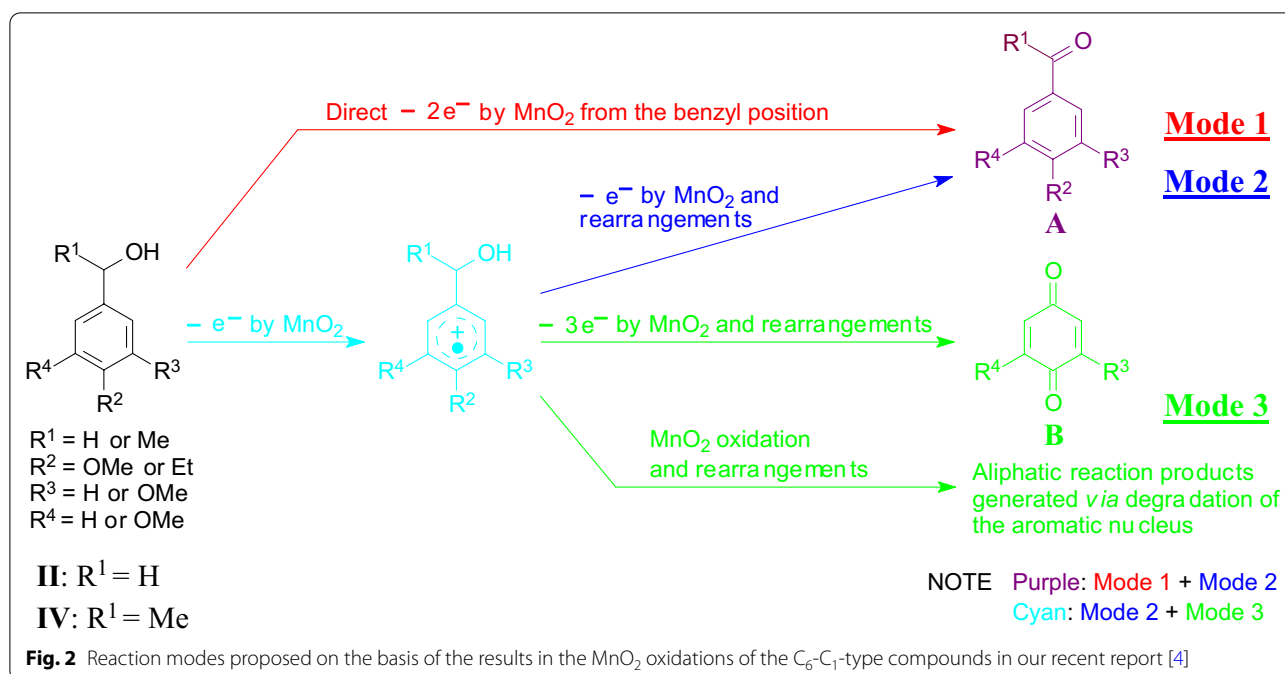1-1-1 Yayoi, Bunkyo-ku, Tokyo 113-8657, Japan

was subsequently examined using various non-phenolic lignin model compounds with a *p*-hydroxyphenyl (**H**), guaiacyl (**G**), or syringyl (**S**) nucleus as well as *p*-ethylphenyl (**E**) nucleus, benzene derivatives (**H**-type (I_H), **G**-type (I_G), **S**-type (I_S), and **E**-type (I_E), Fig. 1), benzyl alcohol derivatives (**H**-type (II_H), **G**-type (II_G), **S**-type (II_S), and **E**-type (II_E), Fig. 1), and the corresponding benzyl alcohol derivatives deuterated at the benzyl positions (**H**-type (III_H), **G**-type (III_G), **S**-type (III_S), and **E**-type (III_E), Fig. 1) at a pH of 1.5 and room temperature in our recent report [4]. Compound I_G or I_S is oxidized by MnO_2 to afford the corresponding benzoquinone derivative (B_G or B_S, respectively, Fig. 1) as the only exclusive major product, while compound I_H or I_E is stable. This oxidation mode of MnO_2 was not previously known. Compound **II** or **III** (indistinguishably showing all the types of aromatic nucleus) except for the **S**-type compound is oxidized almost quantitatively to the corresponding benzaldehyde derivatives (**H**-type (A_H or A_H', respectively), **G**-type (A_G or A_G', respectively), and **E**-type (A_E or A_E', respectively), Fig. 1). Compound II_S or III_S affords not only product A_S or A_S', respectively, but also product B_S as the exclusive major reaction product. The rates are dependent on the type of the aromatic nucleus (**G**- > **S**- >> **H**- > **E**-type). On the basis of these observations, three reaction modes are proposed for the MnO_2 oxidation of compound **II** (or **III**) (Fig. 2). Mode **1** is the direct oxidation of their benzyl alcohols to the aldehydes, product **A** (or **A'**). Mode **2** begins with the oxidation of their aromatic nuclei to afford the aromatic cation radical, but ultimately results in the oxidation of the benzyl alcohol to product **A** (or **A'**). Mode **3** begins the same as mode **2**, but results in the oxidative degradation of the aromatic nuclei to form product **B** as well as many minor unidentified aliphatic reaction products. The magnitude of the kinetic isotope

effect, which is estimated from the ratio of the pseudo-first-order rate constant (k_{obs}) of compound **II** to that of compound **III** observed for their disappearances (**H**-type: 4.7, **G**-type: 4.0, **S**-type: 2.7, and **E**-type: 8.6), can be an index of the degree of the contribution of mode **1**. On the basis of these magnitudes, compounds II_H and II_G are suggested to undergo both modes **1** and **2**, with the contribution of mode **2** to the oxidation of the compound II_G generally being slightly greater than to that of compound II_H, although mode **1** is almost exclusive for compound II_E. Compound II_S undergoes all three modes to further decrease the magnitude. In contrast to modes **1** and **2**, progress to mode **3** can contribute to delignification in actual pulp bleaching where MnO_2 oxidation is introduced.

In this paper, monomeric C_6-C_2-type non-phenolic compounds including lignin models, 1-phenylethanol derivatives (**H**-type (IV_H), **G**-type (IV_G), **S**-type (IV_S), and **E**-type (IV_E), Fig. 3) and their deuterated compounds at the benzyl positions (**H**-type (V_H), **G**-type (V_G), **S**-type (V_S), and **E**-type (V_E), Fig. 3), were oxidized by MnO_2 under the same conditions as in our recent report [4]. The obtained results were compared with those in our recent report to examine the effect of the presence of the *β*-methyl groups and whether the contribution of each reaction mode differs in the MnO_2 oxidations between the C_6-C_1- (**II** and **III**) and C_6-C_2-type (**IV** and **V**) compounds.

Although our recent report describes why the **E**-type compounds, which are not lignin models, were applied [4], this reason is included again here. The Hammett's substituent constant (*σ* value) of the ethyl group present at the *para*-positions of the benzyl carbons in the **E**-type compounds, −0.151, is almost the same as the sum of those of the two methoxy groups present at the

Fig. 1 Structure of monomeric C_6-C_1-type compounds used as starting materials and quantified exclusive major reaction products in our recent report [4]

Fig. 2 Reaction modes proposed on the basis of the results in the MnO₂ oxidations of the C_6-C_1-type compounds in our recent report [4]

Fig. 3 Structure of monomeric C_6-C_2-type compounds used as starting materials and quantified exclusive major reaction products in this study

meta- and *para-*positions of the benzyl carbons in the **G**-type compounds: $+0.115 - 0.268 = -0.153$. Therefore, the rates of the **E**- and **G**-types in compound **II**, **III**, **IV**, or **V** will be similar in chemical reactions at the benzyl positions when these reactions are affected only by the electronic effects of these ethyl and methoxy groups locally appearing only at the benzyl positions. When the reactions are also affected, for instance, by the electron density of the π-electron systems of the compounds, the rates will be different. The application of the **E**-type compounds thus makes the discussion deeper than for that lacking this application.

Materials and methods

Materials

All chemicals used in this study except for the compounds synthesized as described below were purchased from FUJIFILM Wako Pure Chemical Industries, Ltd. (Osaka, Japan), Tokyo Chemical Industry Co., Ltd. (Tokyo, Japan), or Sigma-Aldrich Japan K. K. (Tokyo, Japan), and used without further purification. Ultrapure water used in all the experiments was prepared by a generator, Puric-Z (Organo Co., Tokyo, Japan).

Compounds **IV** were commercially available and purified by flash chromatography (Isolera™, Biotage Japan Ltd., Tokyo, Japan) before use. Compounds **V** were synthesized from the corresponding commercially available acetophenone (acetylbenzene) derivatives by reduction with sodium borodeuteride ($NaBD_4$) in ethanol, and purified by flash chromatography before use.

Preparation of MnO_2 for reaction

MnO_2 was prepared from Mn^{2+} by oxygen oxidation under alkaline conditions. The detailed procedures were as described in our previous and recent reports [3, 4]. The prepared MnO_2 was ground into powder in a mortar. The oxidation power of the MnO_2 was 84.9% of the theoretical value.

MnO_2 oxidation reaction

Although the detailed procedures were as described in our previous report [4], the major portions are included below.

All reactions were conducted in a round-bottom glass flask (200 mL) equipped with a magnetic stirrer. A sulfate buffer (0.50 mol/L, pH 1.5) was prepared in advance by mixing sodium sulfate and sulfuric acid solutions (0.50 mol/L each).

The powdered MnO_2 (1.2 mmol: oven-dry basis (oxidation power basis: 1.02 mmol)) was aged in a sulfate buffer solution (50 mL, 0.50 mol/L, pH 1.5) for 120 min in a glass flask at room temperature. Another sulfate buffer solution (10 mL) consisting of the same sulfate components and containing one of the compounds shown in Fig. 2 (60 μmol) as a starting material was added to the sulfate buffer solution containing the MnO_2 powder to initiate the reaction at room temperature. The initial concentrations of the compound and MnO_2 (insoluble solid) were 0.20 and 20 mmol/L, respectively. Each reaction was conducted three times to confirm reproducibility.

Quantification

A specific amount of the reaction solution was withdrawn at prescribed reaction times to quantify the residual starting material and reaction products. The withdrawn solution was rapidly neutralized with an excess amount of a saturated sodium hydrogen carbonate solution, and mixed with methanol containing an internal standard compound (1,2,3-trimethoxybenzene or 3,4-dimethoxybenzaldehyde). The mixture was filtrated with a membrane filter and injected into an HPLC instrument equipped with an ultraviolet–visible (UV–VIS) absorption detector (LC-2010C$_{HT}$, Shimadzu Co., Ltd., Kyoto, Japan) using the absorbance at 280 nm for quantification.

In HPLC analyses, an HPLC column, Luna 5 u C18(2) 100 Å (length: 150 mm, inner diameter: 2.0 mm, particle size: 5.0 μm, Phenomenex, Inc., Torrance, CA, USA), was used at an oven temperature of 40 ℃ with a solvent flow rate of 0.2 mL min^{-1}. The types of solvent and gradients were as follows: for the reactions of the **H**- and **G**-type compounds, the gradient of CH_3OH/H_2O (v/v) was from 30/70 to 40/60 for 30 min, and then maintained for 10 min. For the reactions of compound **IV$_S$**, the gradient of CH_3OH/H_2O (v/v) was from 30/70 to 50/50 for 30 min, and then maintained for 10 min. For the reactions of compound **V$_S$**, the gradient of CH_3OH/H_2O (v/v) was from 30/70 to 65/35 for 30 min, and then maintained for 10 min. For the reactions of the **E**-type compounds, the gradient of CH_3OH/H_2O (v/v) was from 30/70 to 50/50 for 10 min, from 50/50 to 60/40 for 15 min, and then maintained for 10 min.

Results and discussion

Compounds **IV** and **V** were individually oxidized by MnO_2 under the above-described conditions, which were the same as those employed in our recent report [4]. The disappearance of each type of compounds **IV** and formation of all the exclusive major reaction products are illustrated in Fig. 4. The disappearance of each compound approximated to a pseudo-first-order reaction, although the deviations were not very small in the approximations of several compounds. Table 1 lists the pseudo-first-order reaction rate constants (k_{obs}) observed for these disappearances and, as references, for those of compounds **II** and **III** from our recent report [4], with the squares of the correlation coefficients (R^2) in these approximations. Table 1 also lists the ratios between two values of k_{obs}s (k_{obs}(**II**)/k_{obs}(**III**)); this is explained in the "Introduction" section, and will be used in discussing the oxidation mechanism below.

MnO_2 oxidation of 1-phenylethanol derivatives (compound IV)

Compounds **IV** were oxidized at rates in the order of compound **IV$_G$** > **IV$_S$** > > **IV$_H$** > **IV$_E$**. A possible explanation for this order is described in our recent report [4]. The disappearance of compound **IV$_H$**, **IV$_G$**, or **IV$_E$** was, respectively, accompanied by the almost quantitative
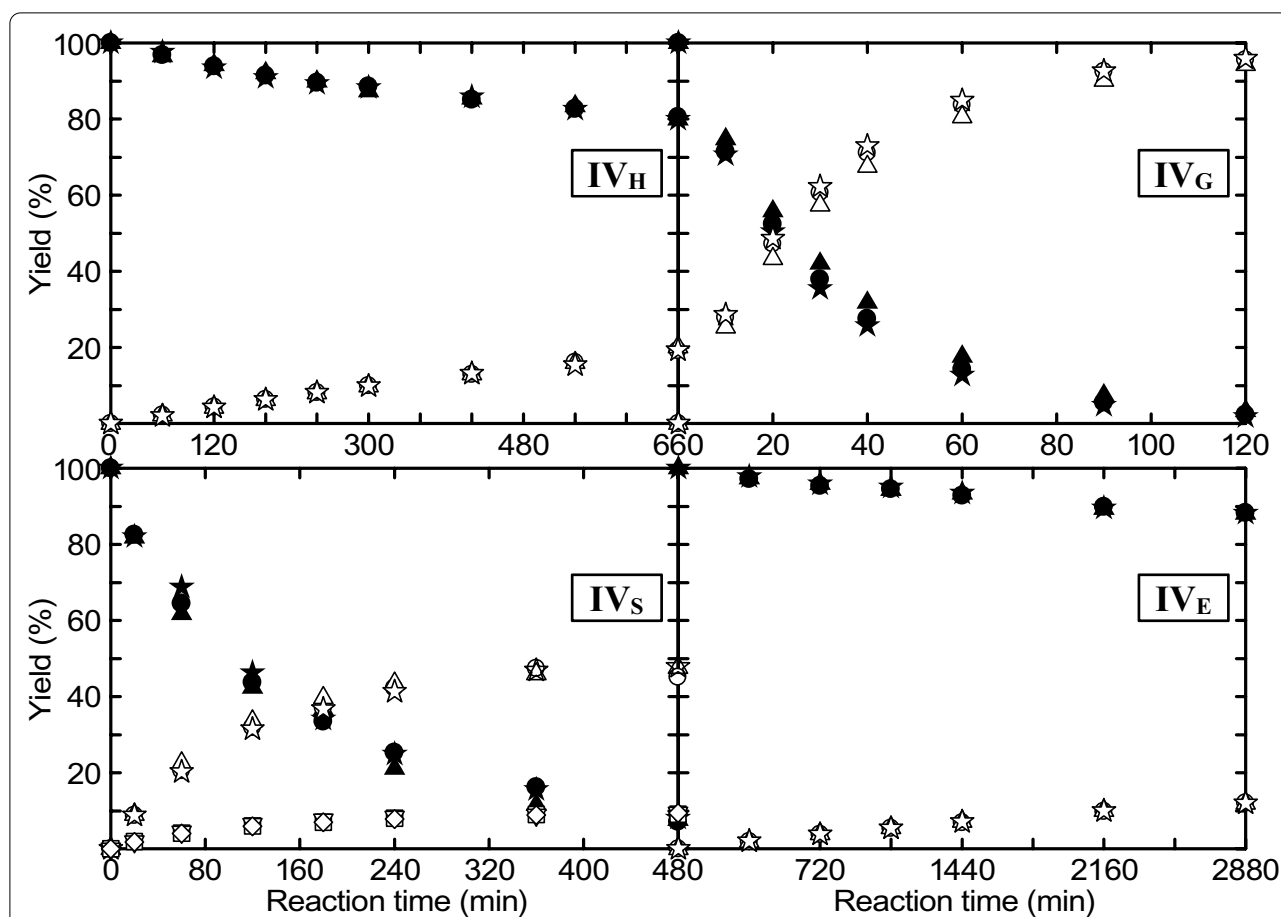
Fig. 4 Time courses of the changes in the recovery yields of compounds **IV** (black marks) and yields of products **C** (white circles, white triangles, and white stars) and **B** (white squares, white inverted triangles, and white diamonds). Upper left: compound **IV_H**, upper right: compound **IV_G**, lower left: compound **IV_S**, lower right: compound **IV_E**. Circles, triangles, and stars indicate the 1st, 2nd, and 3rd trials, respectively, for compounds **IV** and products **C**. Squares, inverted triangles, and diamonds indicate the 1st, 2nd, and 3rd trials, respectively, for products **B**

formation of product C_H, C_G, or C_E (Fig. 3). The oxidation of compound IV_S afforded not only product C_S, but also B_S (Fig. 3) as the only major reaction products, although their formations did not quantitatively accompany the disappearance. The HPLC chromatogram did not show any peak other than those of products C_S and B_S, which indicates that the **S**-nucleus of compound IV_S is degraded to afford ring-opening products. Various types of ring-opening product commonly form without formation of any major product when aromatic nucleus is oxidized and degraded. The **S**-nucleus tends to undergo oxidation to afford ring-opening products more strongly than the other nuclei, owing to high electron density of its aromatic π-electron system. Thus, these results show that oxidation of the benzyl alcohol quantitatively affords product **C** irrespective of whether mode **1** or **2** is followed (Fig. 2), while the aromatic nucleus is degraded and hence unidentified aliphatic reaction products form to deviate the amounts of the detected products from

being quantitative in mode **3**. The contribution of mode **3** in the MnO_2 oxidation of compound IV_S can be calculated by dividing total yield of products via mode **3** by conversion of compound IV_S. The total yield of products via mode **3** can be calculated by subtracting yield of product C_S from conversion of compound IV_S. Thus, the contribution can be calculated to be 49% at a reaction time of 480 min.

These observed phenomena mostly reflect the same tendencies as those in the MnO_2 oxidation of compound **II** in our recent report [4] except that compound **IV** was oxidized more slowly than the corresponding type of compound **II**. This slower rate confirms that the presence of the β-methyl group in compound **IV** decelerates the oxidation owing to the steric factor being larger than that of compound **II**, although the β-methyl group also has an electron-donating inductive effect to accelerate the oxidation. The ratios of the k_{obs} values between compounds **IV** and **II** ($k_{obs}(\mathbf{IV})/k_{obs}(\mathbf{II})$) were 0.25, 0.34, 0.16, or 0.23

Table 1 Pseudo-first-order reaction rate constants (k_{obs}) obtained from three duplicated runs and squared correlation coefficients (R^2) of each run in the MnO_2 oxidation of compounds **IV** and **V** observed in this study and in that of compounds **II** and **III** observed in our recent report [4]

Com.[a]	k_{obs}[b]	R^2	Com.[a]	k_{obs}[b]	R^2	k_{obs}(**II**)/k_{obs}(**III**)
II$_H$	14.7 ± 0.1	0.995	**III$_H$**	3.13 ± 0.09	0.995	k_{obs}(**II$_H$**)/k_{obs}(**III$_H$**) = 4.7
		0.997			0.986	
		0.995			0.987	
II$_G$	911 ± 23	0.999	**III$_G$**	227 ± 8	1.00	k_{obs}(**II$_G$**)/k_{obs}(**III$_G$**) = 4.0
		0.985			1.00	
		0.988			1.00	
II$_S$	343 ± 18	0.962	**III$_S$**	127 ± 2	0.983	k_{obs}(**II$_S$**)/k_{obs}(**III$_S$**) = 2.7
		0.968			0.985	
		0.994			0.983	
II$_E$	2.09 ± 0.06	0.995	**III$_E$**	0.244 ± 0.008	0.961	k_{obs}(**II$_E$**)/k_{obs}(**III$_E$**) = 8.6
		0.992			0.958	
		0.991			0.941	
Com.[a]	k_{obs}[b]	R^2	Com.[a]	k_{obs}[b]	R^2	k_{obs}(**IV**)/k_{obs}(**V**)
IV$_H$	3.66 ± 0.01	0.942	**V$_H$**	0.867 ± 0.013	0.984	k_{obs}(**IV$_H$**)/k_{obs}(**V$_H$**) = 4.2
		0.946			0.982	
		0.939			0.957	
IV$_G$	315 ± 21	1.00	**V$_G$**	96.2 ± 0.7	0.999	k_{obs}(**IV$_G$**)/k_{obs}(**V$_G$**) = 3.3
		1.00			0.998	
		1.00			0.999	
IV$_S$	55.6 ± 2.0	0.984	**V$_S$**	28.9 ± 1.1	0.960	k_{obs}(**IV$_S$**)/k_{obs}(**V$_S$**) = 1.9
		0.978			0.980	
		0.989			0.974	
IV$_E$	0.478 ± 0.008	0.952	**V$_E$**	0.0627 ± 0.0005	0.978	k_{obs}(**IV$_E$**)/k_{obs}(**V$_E$**) = 7.6
		0.968			0.984	
		0.978			0.989	

[a] Abbreviation of compound

[b] Unit: $\times 10^{-4}$ min^{-1}. The values after the '$\pm$' marks are standard deviations obtained from three duplicated runs

for the **H**-, **G**-, **S**-, or **E**-types, respectively, which can be an index of the rate-decreasing effect of the presence of the β-methyl group on the disappearance of compound **IV**. The degree of the rate-decreasing effect of the methyl group in compounds **IV** is thus dependent on the type of aromatic nucleus, although the degrees are not large enough for the order of the disappearance rates of compounds **IV** to differ from that of compounds **II**. This large steric factor of compounds **IV** must affect their reaction modes (Fig. 2), because mode **1** seems most sensitive to the steric factor. The dependence of the reaction modes on the steric factor will be discussed later.

MnO_2 oxidation of deuterated 1-phenylethanol derivatives (compound V)

The observed phenomena were all almost the same as those of compounds **IV** except for the slower disappearances of compounds **V**, which show kinetic isotope effects owing to the presence of the α-deuteriums, and for another phenomenon observed in the oxidation of compound **V$_S$** described below. In the oxidation of compound **IV$_H$**, the recovery yield and yield of product **C$_H$** were $94.3 \pm 0.3\%$ and $5.3 \pm 0.1\%$, respectively, at a reaction time of 660 min ($\pm$ standard deviation calculated from three duplicated runs). The total of these was 99.6%. In the oxidation of compound **V$_G$**, the recovery yield and product **C$_G$** were $31.8 \pm 0.5\%$ and $67.2 \pm 0.4\%$, respectively, at a reaction time of 120 min. The total of these was 99.0%. In the oxidation of compound **V$_S$**, products **C$_S$** and **B$_S$** formed as the exclusive major and secondary prominent reaction products, respectively. The recovery yield and yields of products **C$_S$** and **B$_S$** were $27.7 \pm 1.3\%$, $8.2 \pm 0.2\%$, and $5.3 \pm 0.1\%$, respectively, at a reaction time of 480 min. The total of these was 41.2%. In the oxidation of compound **V$_E$**, the recovery yield and yield of product **C$_E$** were $98.2 \pm 0.1\%$ and

1.5 ± 0.0%, respectively, at a reaction time of 2880 min. The total of these was 99.7%.

The oxidation of compound V_S showed a significant difference from that of compound IV_S. The amount of afforded product C_S was about 1.5 times larger than that of product B_S in the oxidation of compound V_S, while it was about 5 times that of product B_S in the oxidation of compound IV_S (yields of products C_S and B_S at a reaction time of 480 min: 46.8 ± 1.2% and 9.3 ± 0.2%, respectively, Fig. 4). This difference suggests that the oxidation of the **S**-nucleus in compound V_S is competitively and alternatively enhanced by suppressing the oxidation of the benzyl position due to the presence of the deuterium decelerating its abstraction.

Effect of the presence of the β-methyl group on reaction mode

Table 1 lists the ratios of the k_{obs} values between compounds **IV** and **V** with a specific type of aromatic nucleus ($k_{obs}(IV)/k_{obs}(V)$) or between compounds **II** and **III** ($k_{obs}(II)/k_{obs}(III)$) observed in our recent report [4], which is an index of the magnitude of the observed kinetic isotope effect. The magnitude of the kinetic isotope effect is large when the contribution of mode **1**, the direct oxidation of the benzyl alcohol, is large.

The ratio between compounds **IV** and **V** ($k_{obs}(IV)/k_{obs}(V)$) is always smaller than that between compounds **II** and **III** ($k_{obs}(II)/k_{obs}(III)$), regardless of the type of aromatic nucleus, indicating that the presence of the β-methyl group decreases the contribution of mode **1**. The presence of the β-methyl group not only suppresses mode **1**, owing to its steric factor, but also must have the reverse effect to enhance the contribution of mode **1**, as described above. The former effect thus appears more clearly regardless of the type of aromatic nucleus.

Although the ratio between the **E**-type compounds ($k_{obs}(IV_E)/k_{obs}(V_E)$), 7.6, seems large enough to say that these compounds exclusively undergo mode **1**, it is smaller than the ratio of $k_{obs}(II_E)/k_{obs}(III_E)$), 8.6. Therefore, mode **2** contributes at least slightly to the oxidations of compounds IV_E and V_E. The exclusive contribution of mode **1** was presumed for the oxidations of compounds II_E and III_E in our recent report [4], although a slight contribution of mode **2** to the oxidations of these compounds cannot completely be denied.

Conclusions

The disappearance of compound **IV** was in the order of: $IV_G > IV_S >> IV_H > IV_E$ in MnO_2 oxidation. That of compound IV_H, IV_G, or IV_E was accompanied by almost quantitative formation of product C_H, C_G, or C_E, respectively. In contrast, not only product C_S, but also B_S was

produced from compound IV_S as the exclusive major reaction products, but their formation was not quantitative. These phenomena were exactly the same as observed in the same MnO_2 oxidation of compound **II** in our recent report, although the disappearance of a specific type of compound **IV** was slower than that of the corresponding type of compound **II**. It was thus confirmed that the presence of the β-methyl group in compound **IV** decelerates the oxidation owing to the steric factor, although the group should also have an accelerating effect on the oxidation due to the electron-donating inductive effect on the α-carbon.

Authors' contributions
SS conducted the experiments, analyzed the obtained data, and wrote the draft of this manuscript under the supervision of TY. TY completed the final manuscript. SS and TY read and approved the final manuscript. Both authors read and approved the final manuscript.

Availability of data and materials
The datasets used and/or analyzed during the current study are available from the corresponding author on reasonable request.

Declarations

Ethics approval and consent to participate
Not applicable.

Consent for publication
Not applicable.

Competing interests
The authors declare that they have no competing interests.

References
1. Posoknistakul P, Akiho S, Akiyama T, Yokoyama T, Matsumoto Y (2018) Stereo-preference in the degradation of the *erythro* and *threo* isomers of β-O-4-type lignin model compounds in oxidation processes III: in the reaction with chlorine- and manganese-based oxidants. J Wood Sci 64:451–457
2. Dai J, Patti AF, Styles GN, Nanayakkara S, Spiccia L, Arena F, Italiano C, Saito K (2019) Lignin oxidation by MnO_2 under the irradiation of blue light. Green Chem 21:2005–2014
3. Sun S, Akiyama T, Yokoyama T, Matsumoto Y (2020) Utilization of recyclable MnO_2 in prebleaching stage as a catalyst for oxygen delignification or as a delignifying agent. Lignin 1:1–10 (https://www.lignin-society.jp/pdf/lignin1/1-10.pdf)

4. Sun S, Akiyama T, Yokoyama T, Matsumoto Y (2020) Differences in the mechanisms of MnO_2 oxidation between lignin model compounds with the *p*-hydroxyphenyl, guaiacyl, and syringyl nuclei. J Agric Food Chem 68:6819–6825